

## Raman study of $\text{YBa}_2\text{Cu}_3\text{O}_{7-x}$ single crystals grown by a pulling technique: Overdoped, underdoped, and nonsuperconducting state

O. V. Misochko\* and S. Tajima

*Superconductivity Research Laboratory, International Superconductivity Technology Center,  
Shinonome 1-10-13, Koto-ku, Tokyo, 135 Japan*

S. Miyamoto

*Department of Physics, Tokai University, Hiratsuka 259-11, Japan*

H. Kobayashi

*Department of Engineering of Electronic Communications, Meiji University, Japan*

S. Kagiya, N. Watanabe, N. Koshizuka, and S. Tanaka

*Superconductivity Research Laboratory, International Superconductivity Technology Center,  
Shinonome 1-10-13, Koto-ku, Tokyo, 135 Japan*

(Received 12 September 1994)

We have measured the Raman scattering from three single crystals of  $\text{YBa}_2\text{Cu}_3\text{O}_{7-x}$  at high,  $x \rightarrow 0$ , intermediate,  $x \approx 0.5$ , and low doping level,  $x \approx 0.15$ . Both fully symmetrical diagonal and off-diagonal phonons without any disorder induced modes have been identified for  $x \rightarrow 0$ , whereas only diagonal scattering showed substantial strength in the other two crystals. The high frequency of the apical oxygen phonon, reaching  $517 \text{ cm}^{-1}$  at room temperature for  $x \rightarrow 0$ , has been found to be a hallmark of the crystals grown by a pulling technique.

Although high-temperature superconductors have been extensively studied by Raman spectroscopy, and  $\text{YBa}_2\text{Cu}_3\text{O}_{7-x}$  is the best studied material among them, there is still a controversy concerning the origin of Raman forbidden modes (Ref. 1 and references therein). If they originate from the oxygen deficiency, which is supposed to exist primarily in the CuO chains, these additional features should disappear in a pure crystal when  $x$  equals to either zero or unity and there is no disorder in the basal plane. There has been no report on such a perfectly oxygenated (or deoxygenated) crystal up to now. Recently, the IR study of the overdoped  $\text{YBa}_2\text{Cu}_3\text{O}_{7-x}$  crystal grown by a pulling technique has appeared which revealed an unusual  $c$ -axis response.<sup>2</sup> As Raman spectroscopy can provide additional information on charge dynamics and phonon spectrum, here we report on a Raman study of three  $\text{YBa}_2\text{Cu}_3\text{O}_{7-x}$  single crystals with different oxygen content grown by a pulling technique. Features are found indicating uniqueness of the crystals grown by the pulling techniques: At room temperature the frequency of the apical oxygen phonon is higher than that for the crystals grown by other techniques. The  $zz$  component of the “ $B_{1g}$ -like” phonon has been observed in orthorhombic crystals, while no Raman forbidden modes, usually ascribed to disorder, have been seen at any polarization in the overdoped crystal.

The three  $\text{YBa}_2\text{Cu}_3\text{O}_{7-x}$  crystals studied in this work ( $A$ ,  $B$ , and  $C$  hereafter) were grown by a pulling technique.<sup>3</sup> The first crystal  $A$ , a rectangular platelet about  $3 \times 5 \times 1 \text{ mm}^3$  in dimension was cut from the as-grown crystal and annealed in oxygen at  $400^\circ\text{C}$  for 2 months to ensure that the stoichiometry was as close as possible to  $\text{YBa}_2\text{Cu}_3\text{O}_7$ . The crystal had a superconducting transi-

tion of  $89 \text{ K}$  and a transition width of  $0.5 \text{ K}$  measured by four-probe resistivity method, and  $c$ -axis parameter of  $11.68 \text{ \AA}$ . The dc resistivity along  $c$ -direction showed a metallic decrease with cooling that was consistent with the infrared spectra which also revealed an enhancement of the electronic conductivity along the  $c$  axis with reducing temperature for the same crystal.<sup>2</sup> The superlinear temperature dependence and low resistivity,  $\rho_c = 2.5 \text{ m}\Omega \text{ cm}$ , indicated to the high doping level. The in-plane Seebeck coefficient along with the in-plane resistivity were suggested of the overdoped state. The former was negative and the magnitude of the latter was about  $25 \mu\Omega \text{ cm}$  just above  $T_c$  with a negative value when linearly extrapolated to zero temperature.<sup>4</sup> An electron probe microanalysis indicated the ratio among Y:Ba:Cu to equal to 0.970:1.943:3.00 and no trace of impurities such as Al, Mg, and Au. The second crystal  $B$ , a rectangular platelet about  $2.5 \times 3 \times 0.4 \text{ mm}^3$  in size cut from the same as-grown crystal, was put with appropriate amount of  $\text{YBa}_2\text{Cu}_3\text{O}_{7-x}$  ceramic powder into a quartz tube to be evacuated and then warmed up  $600^\circ\text{C}$ . The anneal at this temperature lasted for seven days; after that the crystal had a superconducting transition temperature of  $50 \text{ K}$ , and a transition width of  $10 \text{ K}$  as measured by superconducting quantum interference device magnetometer and  $c$ -axis parameter of  $11.77 \text{ \AA}$ . The third crystal  $C$  obtained from annealing in an inert gas atmosphere for 10 days was nonsuperconducting and tetragonal with lattice parameters of  $c = 11.82$  and  $a = 3.86 \text{ \AA}$ . All Raman measurements were performed at room temperature using a microprobe T64000 equipped with a CCD detector in a backscattering configuration. A laser spot of about  $1 \mu\text{m}$  was produced by a  $\times 90$  objective with a numerical aper-

ture of 0.7. Incident power of the different lines of Ar<sup>+</sup> laser was kept below 0.3 mW. All the crystals had a mirrorlike *ac* face produced by polishing with Al<sub>2</sub>O<sub>3</sub> powder.

Figure 1 shows the Raman spectra of crystal *A* at different polarization geometry. As is well known, there are 15 Raman-active phonons for YBa<sub>2</sub>Cu<sub>3</sub>O<sub>7-x</sub>.<sup>5</sup> Five of them are diagonal modes of *A<sub>g</sub>* symmetry, and the other ten are off-diagonal of *B<sub>2g</sub>* and *B<sub>3g</sub>* symmetry. The diagonal phonons appear in the polarized *zz* and *xx* spectra at 123 (117), 154, 350 (339), 438, and 517 cm<sup>-1</sup>, respectively. No trace of any defect-induced modes or two-phonon feature was seen in the frequency range extended up to 2000 cm<sup>-1</sup> (not shown here). The (O)2-(O)3 and Ba phonons have been observed to have an asymmetric line shape, due to their interaction with an electronic continuum for light polarized within the planes, while the interaction became weaker for the *zz* polarization, resulting in a more symmetric line shape accompanied by an increase in frequency (117→123 and 339→350 cm<sup>-1</sup>, respectively). The spectrum, obtained in the polarization permitting off-diagonal modes, reveals the features at 138, 153, 209, 307, and 588 cm<sup>-1</sup>.

As oxygen content is decreased the spectra drastically change; see Fig. 2. We ascribe these spectra to the ortho-II phase with alternating full and empty chains and concentrate here on the apical oxygen frequency. The full assignment will be given elsewhere.<sup>6</sup> This frequency of the apical oxygen mode for given oxygen content is higher than that previously reported, 499 instead of 484 cm<sup>-1</sup>.<sup>7</sup>

Figure 3 shows the spectra when the oxygen content is further reduced. One can see that the main differences of the crystal *C* spectra as compared to those of the crystal *B* are the following: (1) Increase of the intensity for the

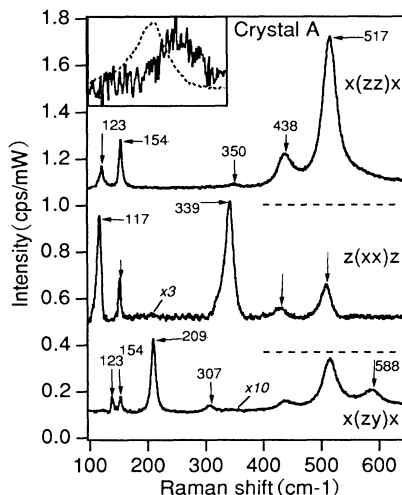


FIG. 1. Raman spectra of the overdoped YBa<sub>2</sub>Cu<sub>3</sub>O<sub>7</sub> single crystal obtained at room temperature. Excitation wavelength 514 nm. Baseline for the bottom spectrum (off-diagonal) is the *x* axis, baselines for the two top spectra (*xx* and *zz*, respectively) are shown in dashed lines. The inset shows a comparison of the *zz* and *xx* component for the (O)2-(O)3 phonon illustrating different line shapes. For clarity, the intensity of the *xx* component was scaled to that of the *zz* one.

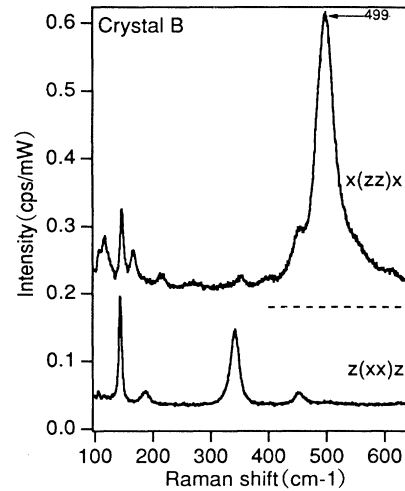


FIG. 2. Raman spectra of crystal *B* obtained at room temperature. Excitation wavelength 514 nm. Baseline for the bottom *xx* spectrum is the *x* axis, baseline for the top *zz* spectrum is shown in dashed line.

phonon at around 600 cm<sup>-1</sup> with simultaneous decrease of that for low-frequency phonons in the *zz* spectra. (2) Appearance of additional feature at 215 cm<sup>-1</sup> in the in-plane polarization. Here we find again the the apical oxygen frequency being higher than that in the tetragonal crystals prepared by other technique, 486 instead of 475 cm<sup>-1</sup>.<sup>7</sup>

We address the polarized spectra first. For crystal *A* there are three observations that are quite different from previously reported results for the optimally doped crystals with the highest superconducting transition temperature.<sup>5,8,9</sup> First, the phonon peak attributed to apical oxygen is observed at 517 cm<sup>-1</sup>. The fact that this increase was produced by polishing can be ruled out by the experi-

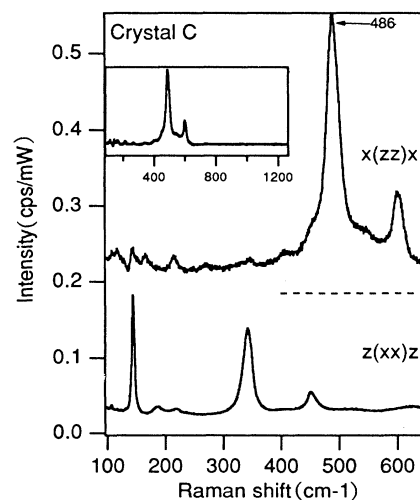


FIG. 3. Raman spectra of crystal *C* obtained at room temperature. Excitation wavelength 514 nm. Baseline for the bottom *xx* spectrum is the *x* axis, baseline for the top *zz* spectrum is shown in dashed line. The inset shows a higher-energy range in the *zz* polarization.

ment done on the surface made by cutting the crystal with a razor blade and the estimates based on the results of the pressure derivative of the oxygen vibrations.<sup>10</sup> Such frequency is extremely high, compared to  $502\text{ cm}^{-1}$  reported in Refs. 5 and 9, which indicates either a larger overlapping between the (O)4- $p_z$  and  $\text{Cu}1-d_{y^2-z^2}$  orbitals, or/and a change in the charge state of apical oxygen. This may, in some way, reflect a decrease in spacing between the  $\text{CuO}_2$  planes and the CuO chains due to a high hole concentration. We note in passing that the line width of the apical oxygen phonon does not exceed that of the Altendorf's study,<sup>8</sup> while the linewidths of the (O)2–(O)3 phonon are substantially smaller,  $20\text{ cm}^{-1}$  instead of about  $30\text{ cm}^{-1}$  in Ref. 8.

The high frequency of the apical oxygen vibration, which is known to be sensitive to oxygen content, strongly supports that the overall oxygen content in our crystal is higher than that for the “fully oxygenated” crystals previously reported. While we had no reliable procedure to determine the absolute oxygen content we made an estimate from the observed correlation between the oxygen deficiency and the value of resistivity at 100 K.<sup>11</sup> This gave  $x=0.025$  for the crystal *A*. Interestingly, the oxygen deficiency for the overdoped crystal of the Altendorf's study,<sup>8,12</sup> estimated in the same way, gave  $x=0.17$ . Given the huge increase in frequency, which twice exceeds the range reported for the ordered orthorhombic crystals spanning from  $497$  to  $503\text{ cm}^{-1}$ , it seems that the electronic properties are very sensitive to small changes just near perfect stoichiometry. Furthermore, such a high frequency is additional evidence for overdoping and hints that this phonon frequency changes rapidly for small changes in the overall oxygen content near  $x=0$ . Note that we observed the similar but reduced in value increase in frequency for the crystals with reduced oxygen content, see Figs. 2 and 3.

In trying to understand the observed shift in frequency we consider it appropriate to recall here the IR Raman study of  $\text{YBa}_2\text{Cu}_3\text{O}_{6.2}$ ,<sup>13</sup> which revealed this phonon at  $507\text{ cm}^{-1}$  instead of  $475\text{ cm}^{-1}$  typical for this oxygen content when probed by the visible Raman. This may be understood assuming that certain electronic states have a vibrational spectrum different from that probed by the visible Raman scattering. If we assume that there is an electronic band formed by the (O)4 orbitals which filling for  $x < 0.05$ – $0.1$  leads to overdoping, we can explain the change in frequency due to alteration of the charge state of the apical oxygen. The presence of the band has been confirmed by the thermoelectric power data.<sup>14</sup>

The second finding is the emergence of the (O)2–(O)3 mode in the  $zz$  polarization for orthorhombic crystals. It seems unlikely to be a “polarization leakage,” because such a leakage would preserve line shape and peak position, which is not the case for our spectra as shown in the inset of Fig. 1. We stress here that this feature, while being extremely weak, was reproducibly detected from different regions of the crystals. This mode, consisting of the out-of-phase displacement of (O)2 and (O)3, has  $B_{1g}$  symmetry in the tetragonal structure. Due to an orthorhombic distortion, the mode changes in symmetry [vibrational amplitudes for the (O)2 and (O)3 become

different] and the polarizability tensor acquires the  $zz$  component. Like the in-phase (O)2+(O)3 mode<sup>15</sup> the out-of-phase (O)2–(O)3 phonon is believed to gain in intensity in the  $zz$  polarization primarily due to mixing with the (O)4 displacement. Within such an approach the intensity for this mode is determined by a dynamic interaction among the (O)2, (O)3, and (O)4 oxygen rather than by a small dimpling of the  $\text{CuO}_2$  planes. Its appearance in our orthorhombic crystals can be interpreted as an increase of such an interaction. The estimates, made in a way similar to Ref. 15, give the admixture of the (O)4 to the (O)2–(O)3 phonon to be around 0.1. The existence of the same feature in the tetragonal crystal *C* may be attributed to photoinduced effect<sup>16</sup> which moves the crystal to a metallic, and thus orthorhombic side. We note that a crucial test for the origin of this feature will be its resonance profile, as it has been done for the (O)2+(O)3 mode,<sup>15</sup> and checking the two-magnon energy range in the tetragonal crystal.

Lastly, we point out the lack of Raman forbidden modes in Fig. 1. Though there is general agreement on the Raman allowed phonons, some differences do appear in the spectra of the different crystals with nominally the same superconducting and structural properties. We know a few Raman studies where additional features, usually ascribed to disorder, have not been reported.<sup>8,17</sup> The most frequently cited are the peaks at  $230$ ,  $575$ , and  $590\text{ cm}^{-1}$  (the first two appear in the  $yy$  and the last in the  $zz$  spectra), which are supposed to become Raman active in the polarized spectra through the disorder in oxygen sublattice.<sup>1,17</sup> In contrast, the crystal under study shows none of these. We can rule out the possibility for these features to appear under more resonant conditions,<sup>18</sup> because even at the most resonant excitation ( $\lambda = 530\text{ nm}$ ) the spectrum was free of them. In addition to the spectral range shown in Fig. 1, we checked carefully the region  $9000$ – $1500\text{ cm}^{-1}$  where second-order Raman scattering was reported.<sup>7</sup> The feature at around  $1050\text{ cm}^{-1}$  was absent in all our crystals. Furthermore, measurement at elevated temperatures, produced by a higher pumping power, showed no additional feature at  $590\text{ cm}^{-1}$  in the  $zz$  polarization for crystal *A*, while for reduced crystals the intensity ratio of defect induced mode to apical oxygen one was independent of pumping power. This may be a signal that even the double-well potential, supposed to be responsible for this feature,<sup>7</sup> does not exist in our crystals. A plausible reason for this seems to be the perfect crystal structure with fewer impurities and less oxygen deficiency in the crystal *A* and ordered vacancies in the reduced crystals.

Next we briefly discuss the off-diagonal phonons shown in Fig. 1. Due to twinning we cannot distinguish between the  $B_{2g}$  and  $B_{3g}$  phonon. Similarly to optimally doped  $\text{YBa}_2\text{Cu}_3\text{O}_{7-x}$ , we find the features at  $138$ ,  $153$ ,  $209$ ,  $307$ , and  $588\text{ cm}^{-1}$  in the depolarized spectrum. Here we point out only that the frequency for the stretching bond vibration appears at  $588\text{ cm}^{-1}$  compared to the previously reported value of  $575\text{ cm}^{-1}$ .<sup>5,9</sup> That is an additional indication of the overdoping that is known to strengthen the Cu–O bond in the  $\text{CuO}_2$  plane. Moreover, substantial differences from the previous studies<sup>5,9</sup> are revealed in the

intensity ratio between the polarized and depolarized spectra,  $I_{zz}/I_{zx}$ . In contrast to the previous studies, where the ratio reached about 100, it shows an order of magnitude decrease down to 10. A comparison with the spectra of the ortho-II crystal with alternating empty and full chains revealed that this change in the intensity ratio was primarily due to alteration of the off-diagonal component intensity.

It is emphasized that the single crystals of the present study are of high quality in the sense of their perfect crystal structure. We suppose that differences in the Raman scattering for our crystal *A* and the crystals with highest  $T_c$  are accounted for by differences in the carrier concentration. This was achieved through a long anneal and through a reduced disorder in both the cation and anion sublattices that enabled the chains to dope the system more effectively. While the superconducting transition temperature is not very sensitive to the overall oxygen content near  $x=0$ , this is not the case, as demonstrated by this study, for Raman scattering. Note that some physical properties such as electronic specific heat<sup>19</sup> and thermal conductivity<sup>20</sup> are highly sensitive to the oxygen content at high doping level, too. In trying to explain the overdoping, we may contemplate the following scenario. With decreasing  $x$  the apical oxygen comes closer to the  $\text{CuO}_2$  plane due to a partial occupation of the  $\text{Cu}2d_{z^2}$  orbital by a hole. Until the  $\text{Cu}2d_{x^2-y^2}$  orbital lies higher than the  $z^2$  one, further doping leads to an increasing

contribution of the  $z^2$  orbital and higher  $T_c$ . When, due to an enhanced Coulomb interaction, the reverse splitting of the  $z^2$  and  $x^2-y^2$  orbitals occurs,<sup>21</sup> further doping goes on to increase the weight of the  $z^2$  orbital, as evidenced by a rapid increase in frequency for the apical oxygen mode, while  $T_c$  starts to decrease. Within such a scenario the overdoping might correspond to the reverse crystal-field splitting. In  $\text{YBa}_2\text{Cu}_3\text{O}_{7-x}$ , the ability of the chain to supply carriers depends largely on the local oxygen ordering.<sup>22</sup> Therefore, it may only be possible to overdoped crystals with an ordered structure. Thus, both the perfect ordering and overall oxygen content are responsible for overdoping.

In summary, both the diagonal and off-diagonal phonons have been measured for an overdoped single crystal of  $\text{YBa}_2\text{Cu}_3\text{O}_7$ . The high frequency for the apical oxygen phonons has been shown to be a specific feature of the crystals grown by a pulling technique. Additionally, the  $zz$  component of the  $B_{1g}$ -like phonon has been detected in orthorhombic crystals.

The authors gratefully acknowledge J. Ricketts for critical reading of the manuscript and Y. Yamada and Y. Shiohara for their help in sample preparation. We are also indebted to M. Badaye for help in measuring of the unit-cell parameters. This work was supported by NEDO for the R&D of Industrial Science and Technology Frontier Program.

\*Permanent address: Institute of Solid State Physics, Russian Academy of Sciences, 142432 Chernogolovka, Russia.

<sup>1</sup>K. F. McCarty, J. Z. Liu, Y. X. Jia, R. N. Shelton, and H. B. Radousky, *Physica C* **192**, 331 (1992).

<sup>2</sup>J. Schützmann, S. Tajima, S. Tanaka, and S. Miyamoto, *Phys. Rev. Lett.* **73**, 174 (1994).

<sup>3</sup>Y. Yamada and Y. Shiohara, *Physica C* **217**, 182 (1993).

<sup>4</sup>I. Terasaki, Y. Sato, S. Tajima, S. Miyamoto, and S. Tanaka, *Physica C* (to be published).

<sup>5</sup>K. F. McCarty, J. Z. Liu, R. N. Shelton, and H. B. Radousky, *Phys. Rev. B* **41**, 8792 (1990).

<sup>6</sup>O. V. Misochko, S. Tajima, S. Miyamoto, and N. Koshizuka, *Solid State Commun.* **92**, 877 (1994).

<sup>7</sup>L. V. Gasparov, V. D. Kulakovskii, E. Ya. Sherman, and V. B. Timofeev, *Sov. Phys. JETP* **73**(5), 929 (1991).

<sup>8</sup>E. Altendorf, X. K. Chen, J. C. Irwin, R. Liang, and W. N. Hardy, *Phys. Rev. B* **47**, 8140 (1993); **48**, 10 530 (1993).

<sup>9</sup>L. V. Gasparov, V. D. Kulakovskii, O. V. Misochko, and V. B. Timofeev, *Physica C* **157**, 341 (1989).

<sup>10</sup>V. D. Kulakovskii, O. V. Misochko, V. B. Timofeev, M. I. Erements, E. S. Itskevich, and V. V. Struzhkin, *Sov. JETP Lett.* **47**, 626 (1988).

<sup>11</sup>H. Claus, M. Braun, A. Erb, K. Röhberg, B. Runtsch, H. Wühl, G. Bräuchle, P. Schweib, G. Müller-Vogt, and H. v.

Löhneysen, *Physica C* **198**, 42 (1992).

<sup>12</sup>R. Liang, P. Dosanjh, D. A. Bonn, D. J. Baar, J. F. Carolan, and W. N. Hardy, *Physica C* **195**, 51 (1992).

<sup>13</sup>V. N. Denisov, C. Talianni, A. G. Mal'shukov, V. M. Burlakov, E. Schönherr, and G. Ruani, *Phys. Rev. B* **48**, 16 714 (1993).

<sup>14</sup>J. L. Cohn, E. F. Skelton, S. A. Wolf, and J. Z. Liu, *Phys. Rev. B* **45**, 13 140 (1992).

<sup>15</sup>O. V. Misochko, E. I. Rashba, E. Ya. Sherman, and V. B. Timofeev, *Phys. Rep.* **194**, 387 (1990).

<sup>16</sup>G. Yu and A. J. Heeger, *Int. J. Mod. Phys. B* **7**, 3751 (1993).

<sup>17</sup>V. G. Hadjiev, C. Thomsen, A. Erb, G. Müller-Vogt, M. R. Koblichka, and M. Cardona, *Solid State Commun.* **80**, 643 (1991).

<sup>18</sup>D. R. Wake, F. Slakey, M. Klein, J. P. Rice, and D. M. Ginsberg, *Phys. Rev. Lett.* **67**, 3728 (1991).

<sup>19</sup>J. W. Loram, K. A. Mirza, J. R. Cooper, and W. Y. Liang, *Phys. Rev. Lett.* **71**, 1740 (1993).

<sup>20</sup>J. L. Cohn, S. A. Wolf, T. A. Vandera, V. Selvamanickam, and K. Salama, *Physica C* **192**, 435 (1992).

<sup>21</sup>D. I. Khomskii and E. I. Neimark, *Physica C* **173**, 342 (1993).

<sup>22</sup>A. Latge, E. V. Anda, and J. L. Moran-Lopez, *Phys. Rev. B* **42**, 2543 (1990).